

2011

# The Density Broadening in a Sodium $F=2$ Condensate Detected by a Pulse Train

Jianing Han  
*Hollins University*

Follow this and additional works at: <https://digitalcommons.hollins.edu/physfac>



Part of the [Physics Commons](#)

---

## Recommended Citation

Han, Jianing. "The density broadening in a sodium  $F=2$  condensate detected by a pulse train." *AIP Advances*, 1, 032106 (2011).  
Hollins Digital Commons. Web. DOI:<http://dx.doi.org/10.1063/1.3621721>.

This Article is brought to you for free and open access by the Physics at Hollins Digital Commons. It has been accepted for inclusion in Physics Faculty Scholarship by an authorized administrator of Hollins Digital Commons. For more information, please contact [lvilelle@hollins.edu](mailto:lvilelle@hollins.edu), [millerjc@hollins.edu](mailto:millerjc@hollins.edu).

## The density broadening in a sodium $F=2$ condensate detected by a pulse train

Jianing Han<sup>1,2</sup>

<sup>1</sup>Joint Quantum Institute, University of Maryland, College Park, MD 20742, USA

<sup>2</sup>Physics department, Hollins University, P. O. Box 9707, Roanoke, VA 24020-1707, USA

(Received 19 April 2011; accepted 28 June 2011; published online 21 July 2011)

The dipole-blockaded sodium clock transition has been detected by high resolution microwave spectroscopy, the multiple-pulse spectroscopy. This spectroscopic technique has been first used to detect the density broadening and shifting in a Sodium Bose Einstein Condensate (BEC) by probing the sodium clock-transition. Moreover, by narrowing the pulse-width of the pulses, some of the broadening mechanisms can be partially reduced. The results reported here are essential steps toward the ground-state quantum computing, few-body spectroscopy, spin squeezing and quantum metrology. *Copyright 2011 Author(s). This article is distributed under a Creative Commons Attribution 3.0 Unported License.* [doi:[10.1063/1.3621721](https://doi.org/10.1063/1.3621721)]

One of the applications of the spin mixture, especially the nuclear spin mixture, is the dipole blockade. The dipole blockade is generally described as the excitation of one atom suppressing the excitation of neighboring atoms, which is promising for quantum gates. Quantum gates can be easily realized in Rydberg states.<sup>1-4</sup> However, the electric dipole-dipole induced collisions between Rydberg atoms limit the lifetime of this type of quantum gates. To increase the lifetime of the Rydberg state, dressed Rydberg states have been proposed to solve the short lifetime issue.<sup>5</sup> However, the amount of Rydberg signal mixed in the ground state is small. Therefore, the ground state atoms are the natural choice for this type of gate. MIT's sodium clock transition data<sup>6</sup> show that this is feasible for the ground state atoms. Here we show that even at very low density, the many-body excitation suppression has been observed.

The Rabi line shape is generated by a single pulse and Ramsey fringes are produced by two pulses. In this experiment, we measure the density broadening by a multipulse technique, which reduces some of the broadening mechanisms as discussed later in this article. The experimental results are compared with our calculations. Specifically, we use a microwave pulse train to detect the line broadening of the sodium  $F=2$  condensate. The experimental data not only show frequency broadening but also a frequency-shift.

If there are no other dephasing processes, the narrower spectrum line can be achieved by increasing the length of the microwave pulse, which can be predicted by the Fourier transform of a single pulse. However, collisions, power instability, and other broadening due to the dephasing over time<sup>7</sup> in the system cause a greater linewidth than the Fourier transform limit of a single pulse, which makes the measurements difficult. The specific broadening mechanism remains unknown. We reduce the linewidth by using a pulse train, which produces a significantly narrower linewidth than the density broadened linewidth. For instance, to simplify the problem, we consider a Rabi sequence and a Ramsey sequence and both have the same total length. Due to the fact that the scattering length of the  $F=2$  state is greater than the  $F=1$  state and collisions are density dependent, the second half population transfer will have a greater effect than the first half population transfer. As the Rabi pulse continuously transfer the second half population to the excited state, the collisions happen faster and faster due to the increasing density of the  $F=2$  state, while in the Ramsey sequence the collision rate remains constant due to the constant density of the  $F=2$  state. By the end of the Ramsey sequence, the second half population is transferred to the  $F=2$  state right before the detection. Therefore, the overall collision rate in the Rabi sequence is greater than the Ramsey sequence.



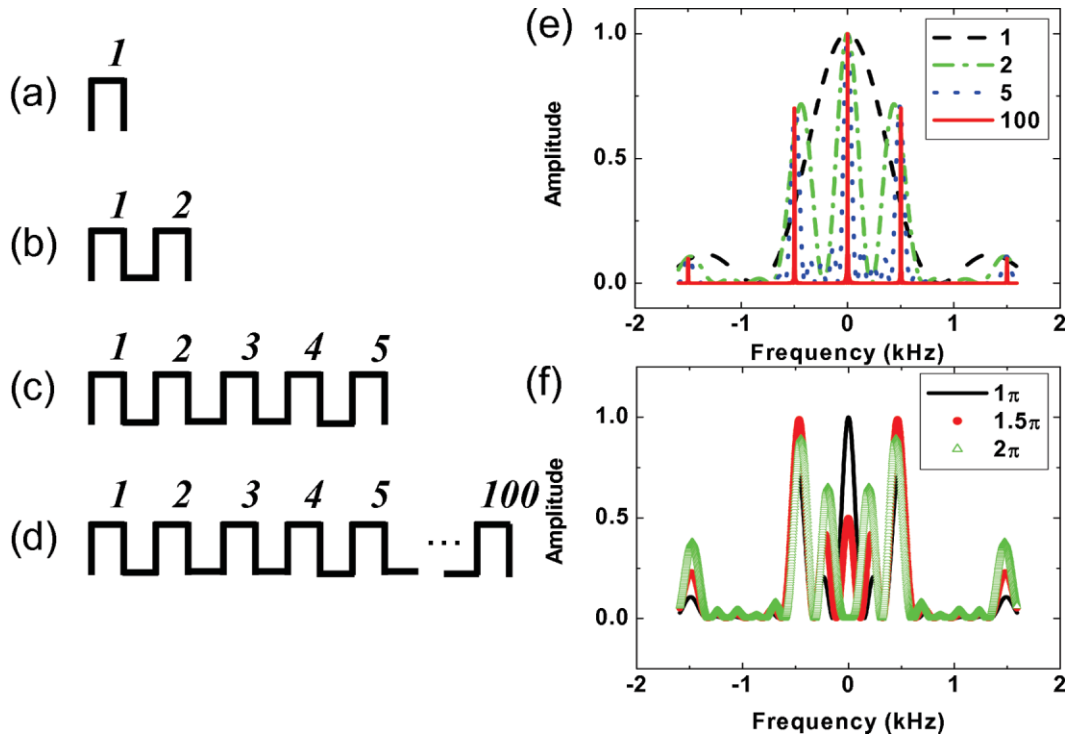


FIG. 1. (Color online) (a)-(e) represent the number of microwave pulses and the shape of the pulses. (a) A Rabi pulse; (b) The Ramsey sequence; (c) Five pulses; (d) 100 pulses. (e) The calculated intensity as a function of the frequency detuning,  $\omega$ . The number of pulses are labeled on the top right of this plot. 1 pulse [(- - -), black dashed line]; 2 pulses [(- · · · -), green dashed-dotted line]; 5 pulses [(· · ·), blue dotted line]; and 100 pulses [(—), red solid line]. (f) The excitation probabilities calculated at three different powers using the five-pulse train as shown in (c). The powers are given in terms of the area under five pulses:  $1\pi$  [(—), black solid line],  $1.5\pi$  [(•), red dot] and  $2\pi$  [(△), green triangle].

This article is arranged in the following way. The multipulse theory is described in the next section, which is followed by the experimental procedures. The experimental results, the excitation suppression and the density broadening caused by the few-body interaction of the sodium clock transition, are then illustrated.

We assume the single-mode approximation is correct. In other words, all the atoms are trapped in the ground angular momentum state of a given potential and the probability of atoms occupying the higher angular momentum modes is negligible. To be consistent with the data we presented in this article, we further assume the duration of the microwave pulse is equal to the time interval between pulses as shown in Fig. 1. In both our calculation and experiments, more general cases, the unequal intervals, are achievable.

A Rabi line shape is generated by a single pulse with a pulse length  $\tau$  and the result linewidth is  $w = \frac{1}{\tau}$ . Ramsey fringes are produced by two pulses with the pulse length  $\tau$  and the time interval between the two pulses is  $T$ . If the powers of the two pulses are equal and the area of each one of the two pulses is  $\frac{\pi}{2}$ . The  $e^{-1}$  linewidth,  $w$ , of one of the fringes is  $w = \frac{1}{T+2\tau}$  and  $w \approx \frac{1}{T}$  if  $T \gg \tau$ . If we increase the number of pulses to  $N$ , keep the pulse-width as  $\tau$ , the interval between pulses as  $T$ , the total area under the  $N$  pulses as  $\pi$  and each of these pulses has the same power, the  $e^{-1}$  linewidth is  $w = \frac{1}{(N-1)T+N\tau}$ .  $w \approx \frac{1}{(N-1)T}$ , if  $T \gg \tau$ . The frequency spectrum of the pulse train is similar to a frequency comb and the interval between two neighboring teeth of the comb is:  $\frac{1}{T+\tau}$ . In this article, we express the power,  $P$ , in terms of  $\pi$ , and the magnetic field strength,  $B$ , can be estimated from  $B = \frac{P}{N\tau\mu} = \frac{\pi}{N\tau\mu}$ , where  $\tau$  is the length of each pulse of a  $N$ -pulse train, and  $\mu$  is the magnetic dipole-moment calculated from the magnetic dipole-coupling between two states considered. In the experiment, the absolute power at a certain frequency is estimated from the line shape measurements

measured at the lowest density and other powers are derived from the calibrated power and the relative power reading from the microwave source.

This multipulse technique can be calculated by exactly solving the time-dependent two-level Schrodinger equations. We apply the notation used in Ramsey's book.<sup>7</sup> In this article, we will use the dressed state picture. That is, we consider one state as one energy level and the other state plus a photon as the second energy level of the two-level system. Therefore, the phases are slightly different from the calculation introduced in Ramsey's book. We start with a two-level system with wave functions,  $\psi_p$  and  $\psi_q$ . Then at a certain time,  $t$ , the wave function can be written as the superposition of those two states:

$$\Psi(t) = C_p(t)\psi_p + C_q(t)\psi_q, \quad (1)$$

where  $C_p$  and  $C_q$  are the coefficients. According to the time dependent perturbation theory:

$$\begin{aligned} i\dot{C}_p(t) &= be^{i\omega t}C_q(t) \\ i\dot{C}_q(t) &= be^{-i\omega t}C_p(t), \end{aligned} \quad (2)$$

where  $\omega = \frac{(E_p - E_q) - \Omega}{\hbar}$  is the energy detuning and  $\Omega$  is the oscillation frequency of the time dependent perturbation; in our case, it is the microwave frequency.  $E_p$  and  $E_q$  are the energies of two levels:  $p$  and  $q$ . If we have a perturbation:  $H'e^{-i\Omega t}$ . Then  $b$  is the dipole coupling matrix element:

$$b = \frac{H'_{pq}}{\hbar} = \frac{H'_{qp}}{\hbar}, \quad (3)$$

where  $H'_{pq} = \langle \psi_p | H' | \psi_q \rangle$ .

If we consider the atom is initially at the lower state,  $C_p(0) = 1$  and  $C_q(0) = 0$ , the Rabi oscillation equations are derived.<sup>7</sup> A more general solution would be considering the atom initially at the state,  $C_p(t_1)\psi_p + C_q(t_1)\psi_q$ , and calculating the coefficients at the time  $t_1 + T$ :

$$C_p(t_1 + T) = \{ [i \cos \theta \sin(\frac{1}{2}aT) + \cos(\frac{1}{2}aT)]C_p(t_1) + i \sin \theta \sin(\frac{1}{2}aT) \exp^{i\omega t_1} C_q(t_1) \} \exp^{\frac{i}{2}\omega T}, \quad (4)$$

$$\begin{aligned} C_q(t_1 + T) &= \{ i \sin \theta \sin(\frac{1}{2}aT)C_p(t_1) \exp^{-i\omega t_1} + [-i \cos \theta \sin(\frac{1}{2}aT) \\ &+ \cos(\frac{1}{2}aT)]C_q(t_1) \} \exp^{-\frac{i}{2}\omega T}, \end{aligned} \quad (5)$$

where  $\cos \theta = -\frac{\omega}{a}$ ,  $\sin \theta = -\frac{2b}{a}$  and  $a = \sqrt{\omega^2 + 4b^2}$  is the Rabi frequency. Fig. 1(e) shows the transition probabilities at different number of pulses, 1, 2, 5, and 100, where the total area of all the pulses within one scan has the area:  $\pi$ . The horizontal axis is the frequency detuning,  $\omega$ . From this plot, we can see that as the number of pulses increases, the linewidth gets narrower and narrower. Fig. 1(f) shows the power dependence of the microwave scans,  $1\pi$ ,  $1.5\pi$ , and  $2\pi$ . Notice that as the power increases to  $2\pi$ , the central peak goes to zero, which corresponds to a  $2\pi$  rotation in a Bloch sphere. Fourier transform is normally used to estimate the linewidth, which is consistent with the results from our calculation; however, the Fourier transform does not predict the power dependence.

The experimental sequence is the following: we first load atoms slowed by a Zeeman slower in a magneto optical trap (MOT). The quadrupole MOT field is then turned off and we start the 30 ms optical molasses stage, where  $6 \times 10^9$  atoms are cooled to 25  $\mu$ K by the end of the optical molasses phase, then the cooled atoms are loaded into a crossed dipole trap. By the end of the dipole trap stage,  $5.0 \times 10^6$  atoms are loaded in the crossed dipole trap at 52  $\mu$ K. We lower the dipole trap potential by keeping the truncation parameter constant,  $\eta = 5$ ,<sup>8</sup> which is called the forced evaporation stage. At the end of the 6 s ramp,  $10^5$  atoms are condensed in the ground state at the temperature 80 nK with the density  $3.0 \times 10^{13} \text{ cm}^{-3}$ . At the end of the ramp, the vertical trap frequency of the condensate is,  $\sim 200$  Hz, to hold the atoms against the gravity. A few millisecond microwave-pulse train is added to drive the sodium clock transition. After waiting for a time interval, a 2.5 ms small field gradient is then added to separate different spin components. 8 ms is then added to do the time of flight (TOF).

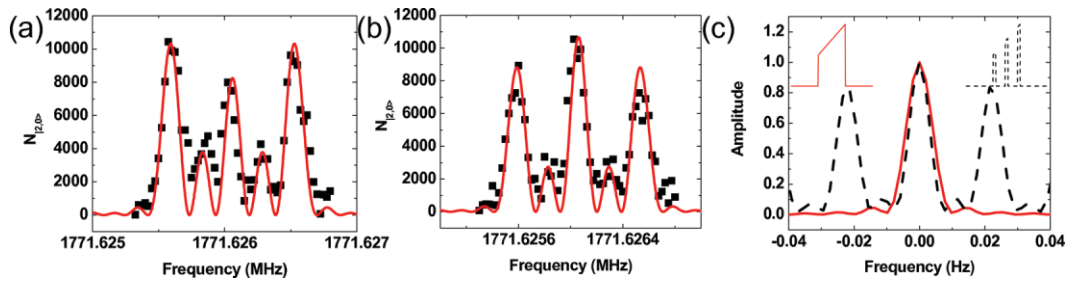


FIG. 2. (Color online) The power dependence measurements with three pulses. This power dependence can be generalized to  $N$  pulses. The black squares (■) are measured data at two different microwave powers and the red solid lines are the calculated transition probabilities by three pulses at two different powers [(—), red solid line]. (a) The power is  $1.33\pi$ . (b) The power is  $1.11\pi$ . In both cases, the pulse-width=the interval between pulses=1 ms. (c) Comparing the single pulse with a continuous power variation [(—), red solid line] and the 3-pulse train with the same power variation [(— — —), black dashed line]. The area under the single pulse and the area under the 3-pulse train are  $\pi$  and the length of the single pulse and the total length of the 3-pulse train are 100 s. The pulse shapes are plotted on the top-left corner, the single pulse, and the top-right corner, a 3-pulse train.

At the end of the TOF, absorption images are taken. The magnetic field is canceled to less than 40 mG.<sup>9</sup>

The power-dependence spectrum of a pulse train is examined. The shape of the spectrum envelope is determined by the total area under the pulse train, or the microwave power. For instance, the envelope width of a  $\pi$  pulse train is  $\sim \frac{1}{\tau}$ . Fig. 2(a) and 2(b) show two microwave scans taken at two different powers,  $1.33\pi$  and  $1.11\pi$ . The data are taken by fixing the microwave power and scanning the microwave frequency. A three-pulse train is used in this case. Here we show two scans taken at two different powers. If the power of the microwave source is continuously varying, using a single pulse will lead to a broadening and using a pulse train will partially reduce this broadening. Fig. 2(c) is the calculation, which shows that the single-pulse with the continuous power variation has a greater linewidth than the 3-pulse train with the same power variation.

The width of individual lines is determined by the total length of the pulse train. Therefore, by fixing the width of a single pulse and the time interval between two neighboring pulses, the longer the pulse train is, the narrower the linewidth is. Figure 3(a) shows two microwave scans taken at two different number of pulses: five pulses, black squares, and three pulses, red circles. The power under each given pulse train is about  $\pi$ . Since the powers of those two scans are low, the power broadening difference in these two scans is negligible. The width ratio between the five-pulse data and the three-pulse data is about:  $\frac{3}{5}$ , which is consistent with the total length ratio of those two pulse trains.

Comparing to the three-pulse data in Fig. 3(a), the five-pulse data shows a significant population drop. The population is reduced by 27%, which is obtained by comparing the peak heights of the 5-pulse data and the 3-pulse data. This indicates a blockade effect in the excited state BEC.<sup>1-4</sup> The solid lines are calculated by taking into account the two-body dipole-dipole interaction with the peak internuclear spacing:  $0.05 \mu\text{m}$ , which is shorter than the typical spacing in a condensate. This indicates that the few-body interaction and higher order multipole-multipole interactions need to be taken into account to quantitatively explain the experimental data. In this calculation, the frequency shift induced by the dipole-dipole interaction is calculated by diagonalizing the matrix composed by  $|10\rangle$ ,  $|2, 0\rangle$  and  $|2, 0\rangle$ ,  $|1, 0\rangle$ , and we also assume that the condensate has the Thomas-Fermi density distribution.<sup>10</sup> The excitation suppression is due to the dipole-dipole broadening detected by a more accurate probe, a probe which has a narrower linewidth than the size of the broadening. To clearly show the dipole-dipole suppression, Fig. 3(b) shows the comparison of the dipole-blockaded excitation and the excitation without the dipole-blockade effect. There are two features about the dipole-blockaded case: first, the peaks are suppressed. Second, the excitation between peaks does not go to zero. The blockade discussions are often confined to two bodies previously; here a many-body system is involved which will introduce more freedoms if it is used in quantum computing. For the two sets of data in Fig. 3(a), the time interval between adding the microwave pulse and the

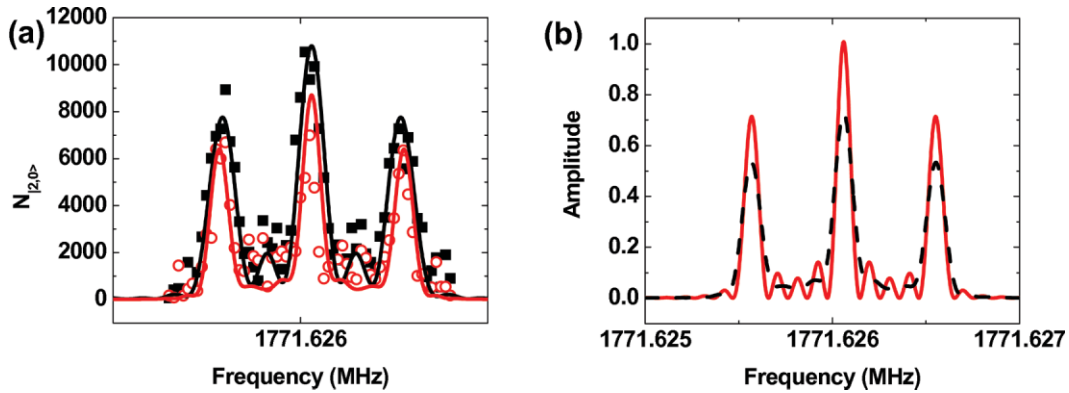


FIG. 3. (Color online) (a) The data are taken with three pulses [(■), black square], the same data as plotted in Fig. 2(b), and five pulses [(○), red circle]. The solid lines are simulations with the dipole-dipole interaction: three pulses [(—), black solid line] and five pulses [(—), red solid line]. Both calculations use  $\pi$  pulses and the amplitudes are rescaled by the number of atoms. In both cases, the pulse-width—the interval between pulses=1 ms and the powers are close to  $\pi$ . Both scans are taken at the same density. (b) The dipole-blockade effect. Both data are calculated with five pulses and the powers are  $\pi$ . The red solid line (—) is calculated without any interactions. In other words, we assume the atoms are isolated. The black dashed line (---) is calculated with the two-body dipole-dipole interaction.

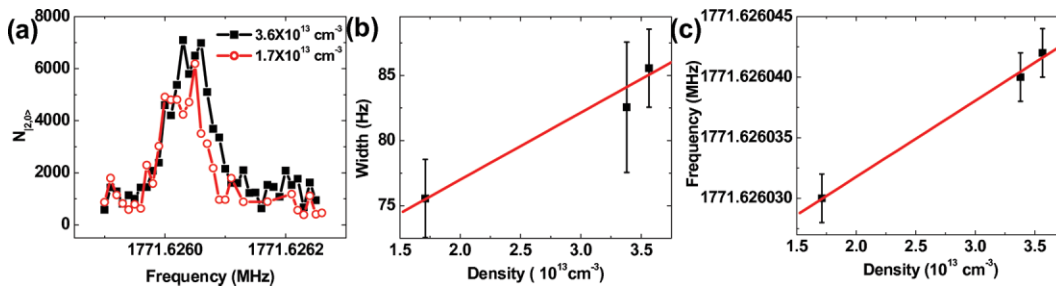


FIG. 4. (Color online) (a) Two microwave scans taken at densities:  $3.6 \times 10^{13} \text{ cm}^{-3}$  and  $1.7 \times 10^{13} \text{ cm}^{-3}$ . The pulse-train used is shown in Fig. 1(c). The microwave scans are taken at the center peak as shown in Fig. 1(f). (b) The Lorentzian fitted linewidth as a function of the atomic density. (c) The peak frequency as a function of the peak atomic density.

TOF detection is fixed; therefore, the atom loss due to the limited lifetime does not play a role in comparing those two sets of data.

Figure 4(a) shows two scans taken at two different densities. A density broadening, to higher frequencies, is observed, which is consistent with the observation made by the MIT group.<sup>6</sup> The linewidth is plotted as a function of the atomic density (Fig. 4(b)), which shows a linear dependence. The density dependent frequency-shift (Fig. 4(c)) shows a linear dependence as well. The error bars are estimated from fitting the microwave scans.

The Doppler frequency shift,  $\Delta\nu = \frac{v}{c}\nu_0$ , of thermal atoms at 100 nK is 0.06 Hz, where  $\Delta\nu$  is the change in frequency,  $\nu$  is the rms velocity of the atoms,  $c$  is the speed of light, and  $\nu_0 = 1.771$  GHz is the transition frequency. If the atoms are condensed to the ground state, the momentum of the condensed atoms can be estimated from calculating the Fourier transform of the many-body wavefunction.<sup>11</sup> The width of the ground state condensate momentum distribution along a given direction,  $x$ , is:  $\Delta p_x \approx 1.58 \frac{\hbar}{x_0}$ , where  $x_0$  is the Thomas-Fermi radius of the condensate. Assuming  $x_0 = 5 \mu\text{m}$ , the lower limit of the Thomas-Fermi radius in our experiment, the width of the Doppler broadening is: 0.005 Hz. In our sample, more than 90% atoms are condensed; therefore, the doppler induced broadening is about 0.005 Hz. The 1D ten-body magnetic dipole-dipole interaction induced frequency broadening is comparable with the broadening that we observed and is three orders of magnitude greater than the Doppler broadening. The detail calculation is very similar to the calculation carried out in Ref. 12. The third broadening mechanism is due to the fact that the frequency-shift depends on the density of the atoms. If there is no interaction between atoms and

the atoms rarely collide with each other, all the particles in the trap should have the same wave-function. However, due to the density dependent interaction, the wave-function is modified by the density. Therefore, due to the nonuniform density distribution, there is a broadening associated with the nonuniform density.<sup>11</sup> The nonuniform density broadening can be calculated from  $\Delta\nu_0 = \sqrt{\frac{8}{147} \frac{nU}{\hbar}}$ , where  $\Delta\nu_0$  is the broadening,  $n$  is the peak density, and  $nU = n \frac{4\pi\hbar^2 a}{m}$  is the chemical potential.  $a$  is the scattering length, and  $m$  is the mass of one sodium atom. The slope of Fig. 4(b), the width vs. the density, is:  $\frac{\Delta\nu_0}{n} = \sqrt{\frac{8}{147} \frac{U}{\hbar}} = 5.5 \times 10^{-18} \text{ m}^3/\text{s}$ . The slope from the experiment is:  $5(2) \times 10^{-18} \text{ m}^3/\text{s}$ , which is quite consistent with the calculation.

The frequency-shift,  $\delta\nu$ , is due to the differential mean-field energy shift between the F=1 state and the F=2 state.<sup>11</sup>

$$\delta\nu = \frac{2n\hbar(a_2 - a_1)}{m}, \quad (6)$$

where  $n$  is the density,  $a_2$  and  $a_1$  are the scattering lengths of the F=2 state and the F=1 state respectively, and  $m$  is the mass of the sodium atom. The measured slope,  $\frac{\delta\nu}{n}$ , of Fig. 4(c) is  $6.3(14) \times 10^{-19} \text{ m}^3/\text{s}$ , which is slightly lower than the calculated slope,  $\frac{2\hbar(a_2 - a_1)}{m}$ , from Eq. (6),  $9.2 \times 10^{-18} \text{ m}^3/\text{s}$ .

In conclusion, we have shown that a pulse train can be used to detect small broadening in a condensate, and the linear frequency broadening and the linear frequency shift of the sodium clock transition as a function of the atomic density in a sodium condensate have been detected by a pulse train. The pulse train calculated from the two-level Schrodinger equations shows the power dependence, which can not be produced by the simple Fourier transform. Moreover, the excitation suppression, which is qualitatively explained by the two-body dipole-dipole suppression, has been observed in the experiment. Finally, the Doppler broadening is negligible. The magnetic few-body dipole-dipole broadening and the nonuniform density broadening are the main broadening mechanisms in this problem.

It is a pleasure to acknowledge the laser cooling and trapping group at NIST.

<sup>1</sup>D. Jaksch *et al.*, *Phys. Rev. Lett.* **85**, 2208 (2000).

<sup>2</sup>M. D. Lukin *et al.*, *Phys. Rev. Lett.* **87**, 037901 (2001).

<sup>3</sup>E. Urban, *et al.*, *Nature Phys.* **5**, 110 (2009).

<sup>4</sup>Alpha Gaetan, *et al.*, *Nature Phys.* **5**, 115 (2009).

<sup>5</sup>J. E. Johnson and S. L. Rolston, *Phys. Rev. A* **82**, 033412 (2010).

<sup>6</sup>M. A. Gorlitz, *et al.*, *Phys. Rev. Lett.* **90**, 090401 (2003).

<sup>7</sup>N. F. Ramsey, *Molecular Beams* (Oxford University Press, New York, 1956).

<sup>8</sup>Wolfgang Ketterle, and N. J. Van Druten, *Advances in Atomic and Molecular Physics* **37**, 181 (1996).

<sup>9</sup>Jianing Han, *et al.*, *Phys. Rev. A* **74**, 054502 (2006).

<sup>10</sup>W. Ketterle, D. Durfee, and D. Stamper-Kurn, *Making, probing, and understanding Bose-Einstein condensates, Proceedings of the International School of Physics - Enrico Fermi* (1999), 67.

<sup>11</sup>J. Stenger, *et al.*, *Phys. Rev. Lett.* **82**, 4569 (1999).

<sup>12</sup>Jianing Han, *Phys. Rev. A* **82**, 052501 (2010).